AD-A274 248

NAVAL POSTGRADUATE SCHOOL
Monterey, California

DTIC
ELECTE
JAN 03 1994
A

S

93-31434

**THE INFLUENCE OF TIG WELDING
THERMAL CYCLES ON HSLA-100 STEEL
PLATE**

Alan G. Fox
Sanjiwan D. Bhole

November 1993

93 12 28 008

NAVAL POSTGRADUATE SCHOOL
Monterey, California

RADM T.A. Mercer
  Superintendent

Harrison Shull
Provost

This report was prepared for and funded by the Welding Branch, Code 2815, Annapolis Detachment, Carderock Division, Naval Surface Warfare Center, Annapolis, MD 21402.

Reproduction of all or part of this report is authorised

This report was prepared by:

A.C. Fox

Alan G. Fox
Associate Professor of Materials Science
Department of Mechanical Engineering

Reviewed by:

Matthew Kelleher

Matthew D. Kelleher, Chairman
Department of Mechanical Engineering

Released by:

J.J. Marto

Paul J. Marto, Dean of Research

REPORT DOCUMENTATION PAGE

Public reporting burden for this collection of information is estimated to average 1 hour per response, including the time for reviewing instructions, searching existing data sources, gathering and maintaining the data needed, and completing and reviewing the collection of information. Send comments regarding this burden estimate or any other aspect of this collection of information, including suggestions for reducing this burden, to Washington Headquarters Services, Directorate for Information Operations and Reports, 1215 Jefferson Davis Highway, Suite 1204, Arlington, VA 22202-4302, and to the Office of Management and Budget, Paper Reduction Project (0704-0188), Washington, DC 20503.

1. AGENCY USE ONLY (Leave Blank)	2. REPORT DATE November 1993	3. REPORT TYPE AND DATES COVERED Technical Report

4. TITLE AND SUBTITLE

The Influence of TIG Welding Thermal Cycles on HSLA-100 Steel Plate

5. FUNDING NUMBERS

N00167-93-WR-30331

6. AUTHOR(S)

Alan G. Fox and Sanjiwan D. Bhole

7. PERFORMING ORGANIZATION NAMES(S) AND ADDRESS(ES)

Department of Mechanical Engineering
Naval Postgraduate School
Monterey, CA 93943

8. PERFORMING ORGANIZATION REPORT NUMBER

NPS-ME-93-008

9. SPONSORING /MONITORING AGENCY NAME(S) AND ADDRESS(ES)

Welding Branch, Code 2815
Annapolis Detachment, Carderock Division
Naval Surface Warfare Center
Annapolis, MD 21402

10. SPONSORING/MONITORING AGENCY REPORT NUMBER

11. SUPPLEMENTARY NOTES

12a. DISTRIBUTION / AVAILABILITY STATEMENT

Approved for Public Release; distribution unlimited

12b. DISTRIBUTION CODE

13. ABSTRACT (Maximum 200 words)

A series of five bead on plate autogenous tungsten-inert-gas (TIG) welds were performed on U.S. Navy HSLA-100 steel. Power variations in these welds was achieved by altering the welding speed, voltage and current and were as follows (in kJ/mm):- 0.7, 1.1, 1.2, 1.6 and 2.2. No evidence was found of either weld metal or underbead HAZ cracking in any of the welds illustrating the advantage of low carbon steel for both weld wire and base plate. Microhardness traverses across both the weld metals and HAZs gave a maximum Vickers diamond pyramid hardness of 345 HV in the coarse grain HAZ next to the fusion line in the lowest power weld; for the highest power weld this was somewhat lower at 328 HV. These are well below 375 which is usually considered to be the lowest Vickers Hardness value for which severe hydrogen induced cold cracking is observed in this type of steel. Optical, scanning and transmission electron microscopy studies of the coarse grain HAZ microstructure in the regions of maximum hardness was correlated with the continuous cooling transformation diagram for this steel and good agreement between observed and predicted microstructures was obtained.

14. SUBJECT TERMS

15. NUMBER OF PAGES
21

16. PRICE CODE

17. SECURITY CLASSIFICATION OF REPORT	18. SECURITY CLASSIFICATION OF THIS PAGE	19. SECURITY CLASSIFICATION OF ABSTRACT	20. LIMITATION OF ABSTRACT
unclassified	Unclassified	Unclassified	Unlimited

ABSTRACT

A series of five bead on plate autogenous tungsten-inert-gas (TIG) welds were performed on U.S. Navy HSLA-100 steel. Power variations in these welds was achieved by altering the welding speed, voltage and current and were as follows (in kJ/mm):- 0.7, 1.1, 1.2, 1.6 and 2.2. No evidence was found of either weld metal or underbead HAZ cracking in any of the welds illustrating the advantage of low carbon steel for both weld wire and base plate. Microhardness traverses across both the weld metals and HAZs gave a maximum Vickers diamond pyramid hardness of 345 HV in the coarse grain HAZ next to the fusion line in the lowest power weld; for the highest power weld this was somewhat lower at 328 HV. These are well below 375 which is usually considered to be the lowest Vickers Hardness value for which severe hydrogen induced cold cracking is observed in this type of steel. Optical, scanning and transmission electron microscopy studies of the coarse grain HAZ microstructure in the regions of maximum hardness was correlated with the continuous cooling transformation diagram for this steel and good agreement between observed and predicted microstructures was obtained.

iii

INTRODUCTION

The US Navy has been developing HSLA steels for shipbuilding applications as replacements for the traditional HY series which are difficult to weld. These HSLA steels have a low carbon content (typically < 0.06% wt.% C) to improve weldability, and microalloying additions of niobium which control austenite grain size during rolling to offset the strength loss due to reduced carbon content. These steels also contain copper additions which increase the strength through precipitation (see, for example, Fox, Mikalac and Vassilaros 1993 and Czyryca, Link, Wong, Aylor, Montemarano and Gudas 1990)

Although these steels exhibit good weldability in terms of their resistance to hydrogen induced cracking, there is potential for loss of offset yield strength in the HAZ and weld metal (if it has the same composition as the base plate) during welding. This could occur as a result of the thermal cycling which could negate the effects of strengthening of the plate due to the final controlled roll pass which does not allow for significant recrystallisation of the austenite and introduces large numbers of dislocations. Since the U.S. Navy requires the complete weldment to meet the parent plate specifications, any mechanical property changes in the weld metal and HAZ associated with welding passes need to be closely studied and understood.

The present work was directed towards the evaluation of the effects of heat input during welding of 25.4 mm thick HSLA-100 plate on the HAZ microstructure and mechanical properties.

EXPERIMENTAL PROCEDURE

Material

The steel used was a 25.4 mm thick plate supplied by the Phoenix Steel Company and conforming to the Navy specification (MIL-S-24645A) for HSLA-100 steel.The steel was made by the electric arc process, aluminum deoxidized and calcium treated to obtain a sulfur level of 0.002 wt.%. The chemical composition of the steel is shown in table 1. The steel was then controlled rolled with the final pass being at a temperature below the recrystallization temperature of the austenite. The rolled plate was then reaustenitized at 900 °C for 60 minutes, water quenched and aged at 675 °C for 75 minutes and finally air cooled to room temperature.

Welding

The welding machine used for the autogenous bead-on-plate TIG welds was a Miller DC Welding Power Source, Model SR600/SCM1A. The vertical and transverse positioning was performed manually, but the longitudinal motion that controls the welding velocity was performed by a motorized traverse. Velocity precision was within 0.05 mm/s. For all welds, a tungsten electrode

with a 45° tip angle and 3.125 mm tip spacing was used. Pure argon was used as the shielding gas, with a flow rate of about 1.573×10^{-4} m^3/s and no preheat was employed.

The plate surface was first cleaned with a wire brush and the plate was positioned on a base table in a horizontal orientation. The electrode was then adjusted to give the necessary tip spacing. The horizontal travel of the torch was set at the required speed setting (based on previously conducted calibration trials). The current dial was set to the required current (either 200 or 250 A) and the arc was struck between the tungsten electrode and the HSLA plate with the aid of a stick electrode. Simultaneously, the horizontal travel of the torch was commenced. The actual current was then obtained by constant adjustment of the dial knob on the power source. The voltage readings which tended to fluctuate with the progress of the weld run were constantly monitored. The voltage readings recorded were taken from the last third of the weld run by which time it was possible to maintain a steady current at the desired level. The horizontal traverse speed was verified by timing the reverse travel of the torch across the length of the plate back to its starting position. This procedure was repeated for the rest of the weld runs with different power settings and speeds as shown in table 2. The power inputs ranged from 0.7 to 2.7 kJ/mm (with an input efficiency of of about 70%). This latter power input is close to what would normally be expected in routine TIG welding.

The weldments were sectioned at a distance of 50 mm from the end of the weld run to examine the through-thickness surface. The sections were then ground, polished and lightly etched with 5 % Nital to outline the various zones of the weldment.

Microhardness profiles of each weldment were then carried out using a Vickers microhardness tester. Measurements were taken radially from the center of the weld in five directions as shown in figures 9 and 10. Next, each weldment was repolished and etched with 5 % Nital for microscopic examination. Selected weld areas were also examined using scanning and transmission electron microscopy (TEM). TEM samples were prepared by cutting 0.2 mm thick slices from the position in the weld of interest and then stamping out 3 mm diameter discs which were ground down to a thickness of 0.0375 mm. TEM foils were prepared from these discs by thinning with a Struers twin jet electropolisher using a 3 % perchloric acid, 35 % butoxy ethanol and 62 % ethanol (by volume) electrolyte at 70 V at a temperature of -30 °C.

Modeling

The model of Adams (1958) which is based on the Rosenthal (1941) theory was used to calculate the cooling time of the coarse grain HAZ for the temperature range 800 °C to 500 °C.

RESULTS

Mechanical Properties

The mechanical properties of the base plate after the quench and temper (aging) treatment are given in tables 3 and 4. It should be noted that there was very little anisotropy in the tensile test data (table 3) mainly due to the very low levels of sulphur (0.002 wt.%) and the calcium treatment during steelmaking which leads to small non-deformable sulfide and oxide inclusions. The Charpy impact data (Table 4) did show some differences between the longitudinal and transverse data but, again, this was not very large. In all cases, the base plate HSLA-100 met the Navy specifications for room temperature off set yield strength of (690 MPa) minimum, and Charpy impact at -19 °C and -84 °C of 80 J and 50 J respectively .

The hardness profiles across the welds were plotted from Vickers microhardness measurements versus distance measured from the fusion line taken as zero for the different heat inputs (figures 1-3). It can be seen that there is a peak value of the hardness in the coarse HAZ very close to the fusion line in each of the measured directions. The peak hardnesses in the HAZ and the weld metal (WM) are a function of heat input as shown in figure 4.

Microstructure

An optical micrograph of the as-received plate is shown in figure 5 and it exhibits a mixture of needle-like and bainitic structure.The SEM micrograph illustrates this structure much better (figure 6). The TEM micrograph in figure 7 shows the martensite/bainite structure which is typical of as-quenched (in water) HSLA-100 steel (for samples taken from near the surface for 25.4 mm plate). It is clear that this is tempered and overaged since the dislocation density is somewhat lower than one would expect in an as-quenched sample and copper precipitates are clearly visible.

Figures 8-10 show low magnification micrographs of three of the five weldments to illustrate the relationship between heat input and weld HAZ size. The orientations of the different hardness profiles measured can also be seen in figures 9 and 10. It should also be noticed that cracking is absent in all these photomicrographs and that neither underbead (HAZ) nor weld metal cracking was evident in any the samples.

The areas of special interest in the present investigation were the coarse grain HAZ next to the fusion line in the weldments. Figures 11 and 12 show the SEM micrographs of the highest and lowest heat input welds (welds 1 and 5) respectively. There is a distinct difference in the size of the martensite/bainite packets and in the lath sizes themselves and as expected these are larger for weld 1 which has the highest heat input. Detailed examination of the two weldment HAZs (welds 1

3

and 5) was carried out in the TEM. Figure 13 shows that the weld 1 (high heat input) HAZ structure comprised granular bainite, both interlath and blocky retained austenite, autotempered carbides (in martensite laths) and some transformation twins. The low heat input weld (weld 5), figure 14, had a predominantly lath martensite structure with interlath retained austenite, autotempered carbides in the laths and far fewer bainitic laths. No copper precipitates were observed in the coarse grain HAZs of either welds 1 and 5 .

DISCUSSION

The main objective of the present study was to determine the effect of weld heat input on the mechanical properties and microstructure of weldments in HSLA-100 steel. It is well known that welding can lead to HAZ embrittlement and hydrogen cracking. In HSLA steels, the HAZ could also exhibit a deterioration in the 0.2% offset yield strength relative to that of the base plate. Such degradation of properties would not be acceptable to Navy specifications which require the weldment to at least retain original strength levels and to avoid embrittlement leading to cracking.

The thermal cycles experienced by the base plate being welded are a function of heat input, plate thickness and thermal characteristics. In the present study the only variable was the heat input. The hardness profiles of the weldments, figures 1 - 3, clearly show a peak in the hardness curve in the coarse HAZ next to the fusion line. The values of the peak hardness vary from 345 to 328 HV over the range of heat inputs from 0.7 to 2.7 kJ/mm respectively. These hardness values clearly indicate that some embrittlement of the weldment has taken place. As discussed by Kirkwood (1987) it is difficult to state a hardness below which a certain steel will not be susceptible to hydrogen induced cold cracking (HIC) since it would seem that this decreases as the carbon equivalent decreases and for very low carbon equivalent steels Kirkwood suggests that hardness values as low as 300 HV may still be too high to avoid HIC. For HSLA-100 steels which are relatively highly alloyed Kirkwood's data indicates that hardness values of 375 HV or less will be sufficient to avoid HIC. This means that the steel studied in the present work is highly weldable without preheat which is confirmed by the absence of any cracks in the weldments. On the other hand, the higher hardness does show that the HAZ tensile strength is greater than that of the base plate, as is the tensile strength of the weld metal. The sensitivity of the HAZ hardness to heat input is highlighted by figure 4 which shows that the peak hardness in the HAZ and the weld metal decreases with increasing heat input as would be expected since cooling rates would naturally decrease with increasing heat input.

An examination of the CCT diagram for HSLA-100 steel (figure 15) shows that hardnesses in the 328-345 HV range are achieved by transformation to a microstructure which is a mixture of

4

martensite and granular bainite. The relative proportions of these will determine the actual hardness. The base plate microstructure, figure 7, shows tempered martensite/bainite with copper precipitation and an average hardness of 278 HV which corresponds to a tensile strength of 123 ksi in good agreement with the data shown in table 3. For the weldment to develop a higher range of hardness in the HAZ, there would have to be a substantially faster cooling rate from the austenitization temperature.

The cooling time at the HAZ/weld metal boundary between 800 to 500 °C was also calculated using the model of Adams (1958) and it was seen that there was a significant difference, 9.56 and 2.62 secs, for welds 1 and 5 respectively. Thus, the low heat input weld 5 experiences a much faster cooling rate through the transformation and ends up with a HAZ hardness of 345 HV which indicates a predominantly martensitic structure, on the CCT diagram. This is confirmed by the TEM micrograph of the HAZ taken close to fusion boundary, figure 14. On the other hand, the high heat input weld 1, with its much slower cooling rate, has a hardess in the HAZ of 328 which indicates a predominantly granular bainite structure with some martensite which is clearly confirmed by the TEM micrograph figure 13 taken from this region. In all cases, autotempered carbides are precipitated in martensite laths. The cooling rates in both these welds are too high for the precipiation of ε-Cu.

The implications of this hardness data for the 0.2% offset yield and tensile strengths of both the weld metal and HAZs are very interesting. The present hardness data indicate that the tensile strengths of both the weld metal (which is also HSLA-100 in this case) and the HAZ are increased by the welding process but the thermal cycling has generated microstructures that are typical of rapid cooling rates similar to quenching (either in water or other media). The tensile test data of the present work indicates that the offset yield strength-to-tensile strength ratio is about 1.0 for overaged (tempered) HSLA-100 plate in agreement with previous work, but for the as-quenched (in water) condition this ratio can be as low as 0.7 (see Czyryca et al. 1990 and Fox et al. 1992). This is clearly the case for the both the weld metal and HAZ for all weldments as the tensile strengths at the fusion line derived from the hardness data are at most between 157 and 166 ksi for the lowest and highest powers respectively. This suggests that the offset yield strengths for this position in these weldments could be as low as between 110 and 116 ksi respectively which is below that of the base plate and if the requirement that the weldment must have the same offset yield strength as the base plate is to be met then a weld wire with a significantly higher offset yield strength in the as-welded condition must be used. This wire would preferably have a low carbon content (< 0.08 wt.% C) but may need to be slightly more highly alloyed than HSLA-100. Alternatively, it may be preferable to accept a strength mismatch between the base plate and the

5

weld metal such that the yield strength of the latter is a few percent lower. In this case the use of a weld wire with a similar carbon and alloying content to the parent could be used and an improved weld metal toughness will be obtained.

REFERENCES

Adams C.M. (1958) Welding Journal AWS, 37 (5), 210.

Czyryca E.J., Link R.E., Wong R.J., Aylor D.A., Montemarano T.W. and Gudas J.P. (1990), Naval Engineers Journal, May 1990, 63.

Fox A.G., Mikalac S. and Vassilaros M.G. (1992) in Gilbert R. Speich Symposium Proceedings edited by G. Kraus and P.E. Repas, The Iron and Steel Society of AIME, Montreal, Quebec, Canada, October 25-28 1992.

Kirkwood P.R. (1987) in Proceedings of an International Symposium on Welding Metallurgy of Structural Steels edited by J.Y. Koo, The Metallurgical Society, Denver, Co, February 22-26 1987.

Rosenthal D. (1941) Welding Journal, 20, 220s.

Wilson A.D., Hamburg E.G., Colvin D.J., Thompson, S.W. and Krauss G. (1988) in Proceedings of Micralloying '88, ASM International, 259.

Table 1 Chemical composition (wt.%) of the HSLA-100 plate and Military specification-24645A for which maximum values are shown if no range is given.

Element	HSLA-100	MIL-S-24645A
C	0.040	0.060
Si	0.260	0.400
Mn	0.810	0.75 - 1.05
Ni	3.550	3.35 - 3.65
Cr	0.550	0.45 - 0.75
Mo	0.480	0.55 - 0.65
Cu	1.480	1.45 - 1.75
Nb	0.031	0.02 - 0.06
P	0.008	0.020
S	0.002	0.006
Al	0.032	

Table 2 Summary of weld run settings

Run #	Current (A)	Voltage (V)	Velocity (mm/s)	Heat Input (kJ/mm)
1	250	15.0	1.40	2.7
2	250	14.6	2.26	1.6
3	200	13.6	2.26	1.2
4	250	15.2	3.55	1.1
5	200	13.0	3.55	0.7

Table 3 Tensile Test Properties of HSLA-100 Plate

	Longitudinal	Transverse
0.2 % Proof Stress, MPa	807	814
Ultimate Tensile Stress, MPa	848	848
Elongation, % (25.4 mm gage length)	25	27
Reduction in Area, %	74	75

Table 4 Charpy V-notch Impact Toughness of HSLA-100 Plate

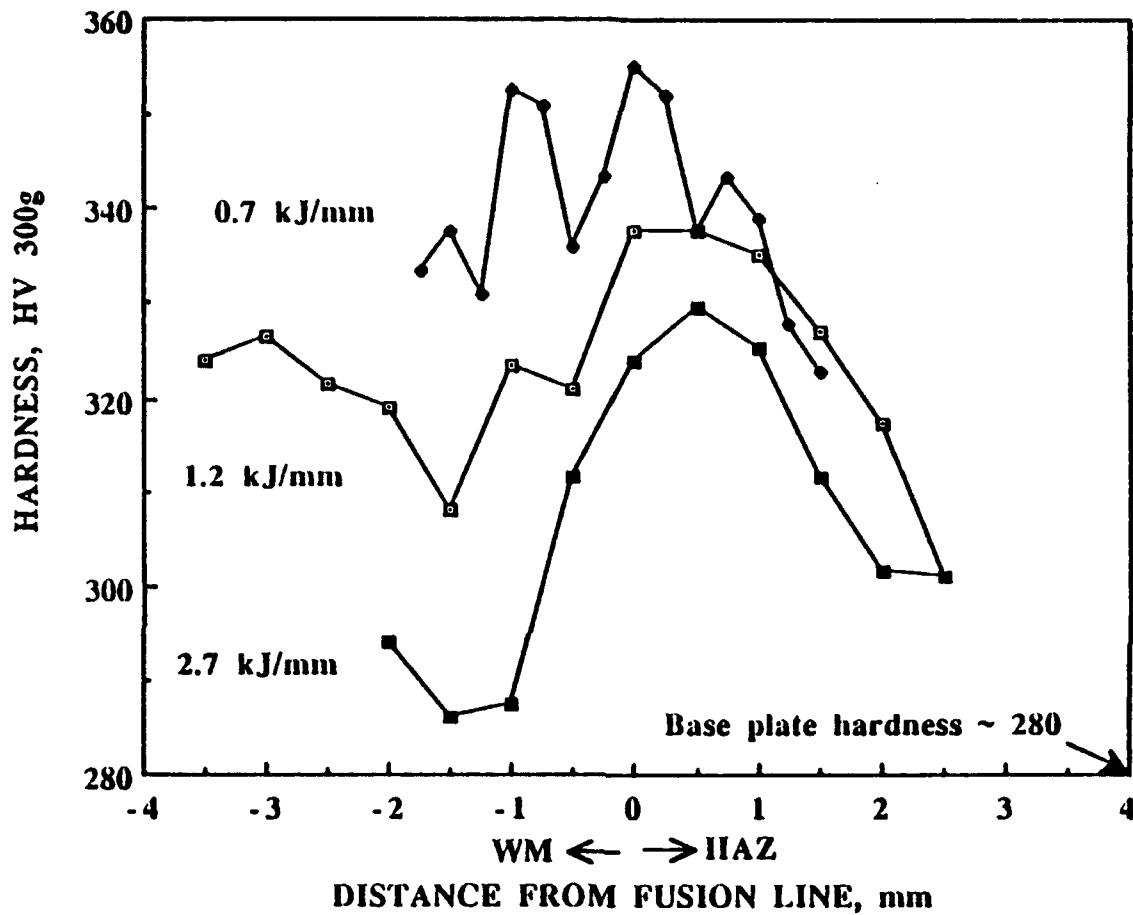| Test Temperature (^{o}C)	T-L Orientation		L-T Orientation	
	Energy (J)	Shear (%)	Energy (J)	Shear (%)
54	202	100	262	100
-18	220	100	250	100
-34	187	100	231	100
-51	190	100	209	100
-84	133	100	184	100
-107	113	10	134	20

Figure 1. Hardness profiles across the weld metals (WM) and HAZs in the horizontal directions for all heat inputs as indicated. These profiles were taken from the weld center as shown in figures 9 and 10 and an average of the measurements for each pass over the fusion zone boundary was taken.
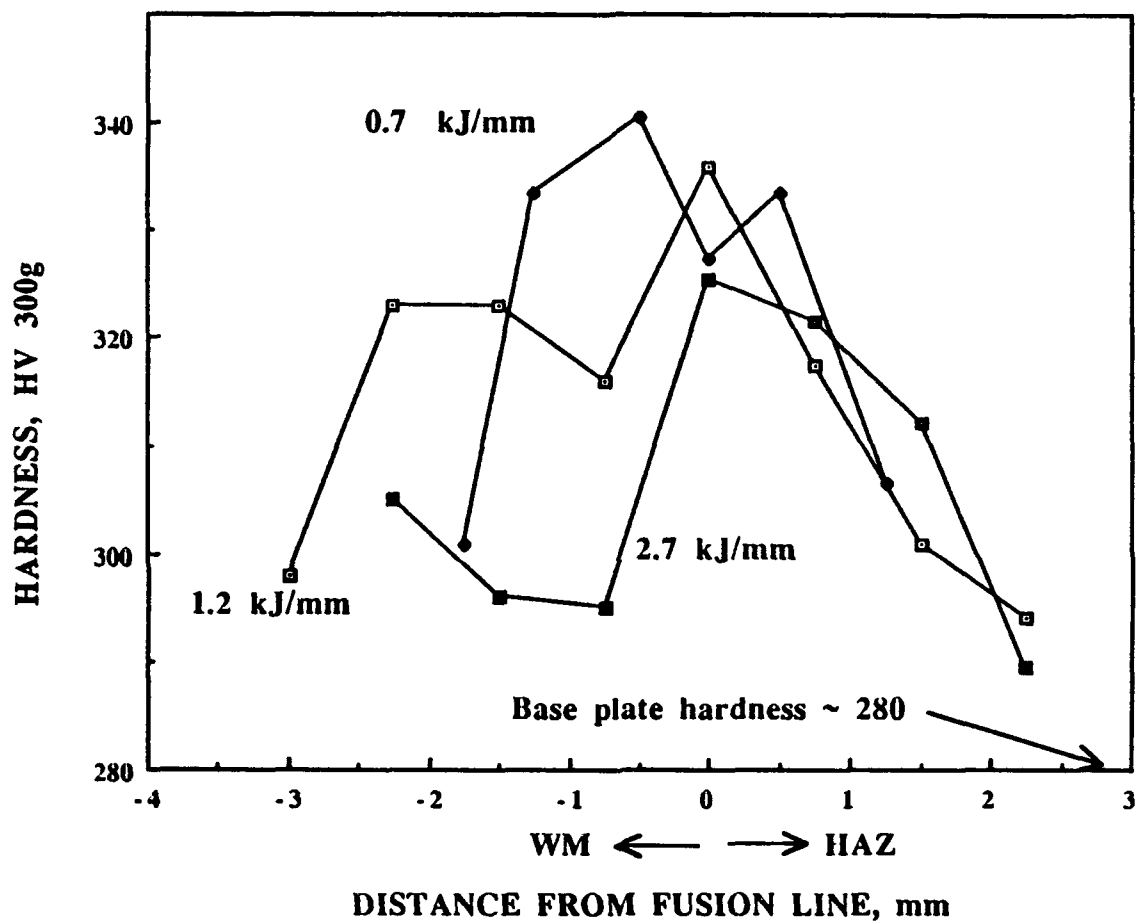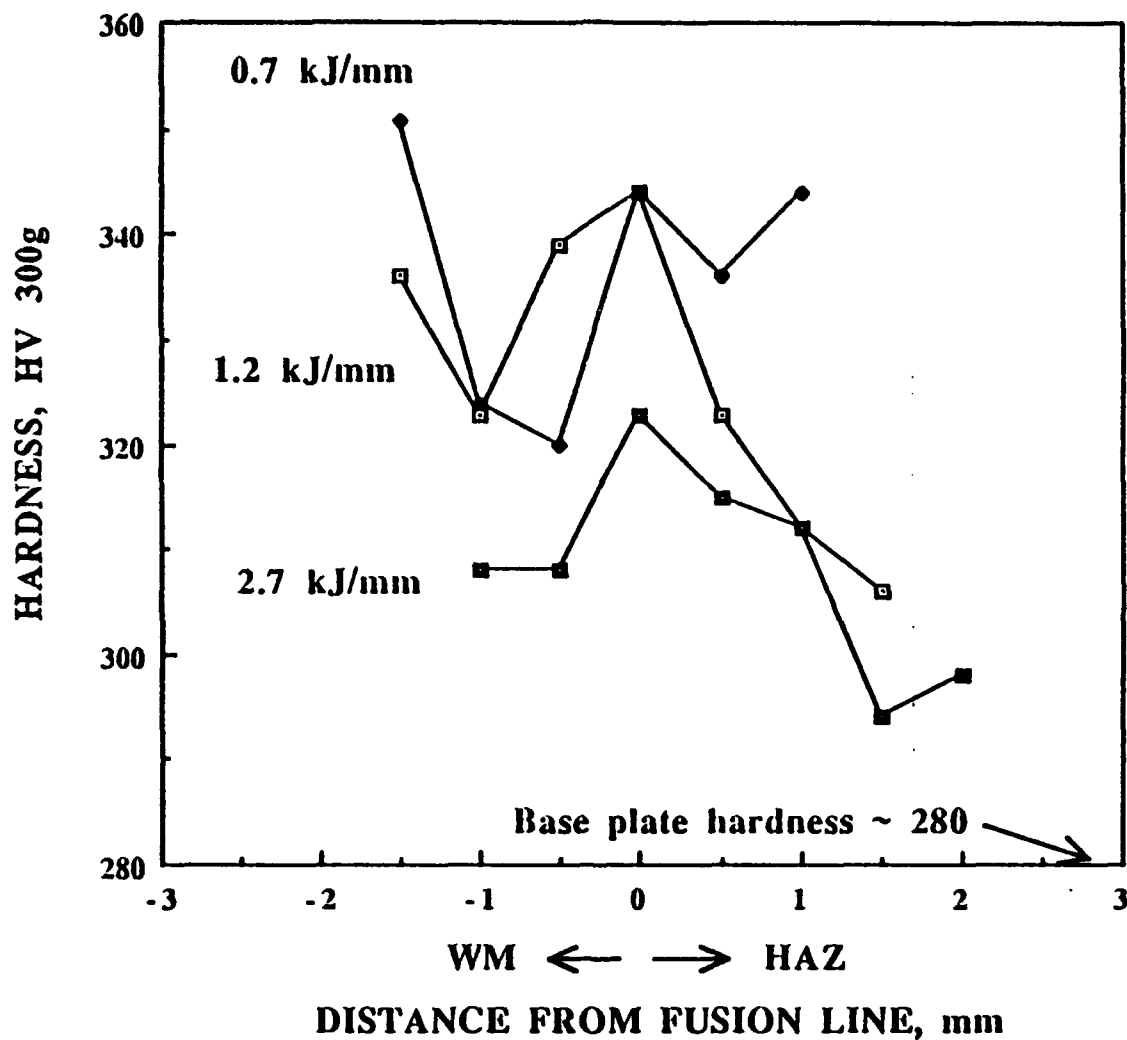
Figure 2. Hardness profiles across the weld metals (WM) and HAZs in the radial directions (45 ° to the horizontal) for all heat inputs. These profiles were taken from the weld center as shown in figures 9 and 10 and an average of the measurements for each pass over the fusion zone bounday was taken.

9

360

0.7 kJ/mm

1.2 kJ/mm

HARDNESS, HV 300g

340

2.7 kJ/mm

320

300

Base plate hardness ~ 280

280
-3   -2   -1   0   1   2   3

WM ← → HAZ

DISTANCE FROM FUSION LINE, mm

Figure 3. Hardness profiles across the weld metals (WM) and HAZs in the vertical directions for all heat inputs. These profiles were taken from the weld center as shown in figures 9 and 10.
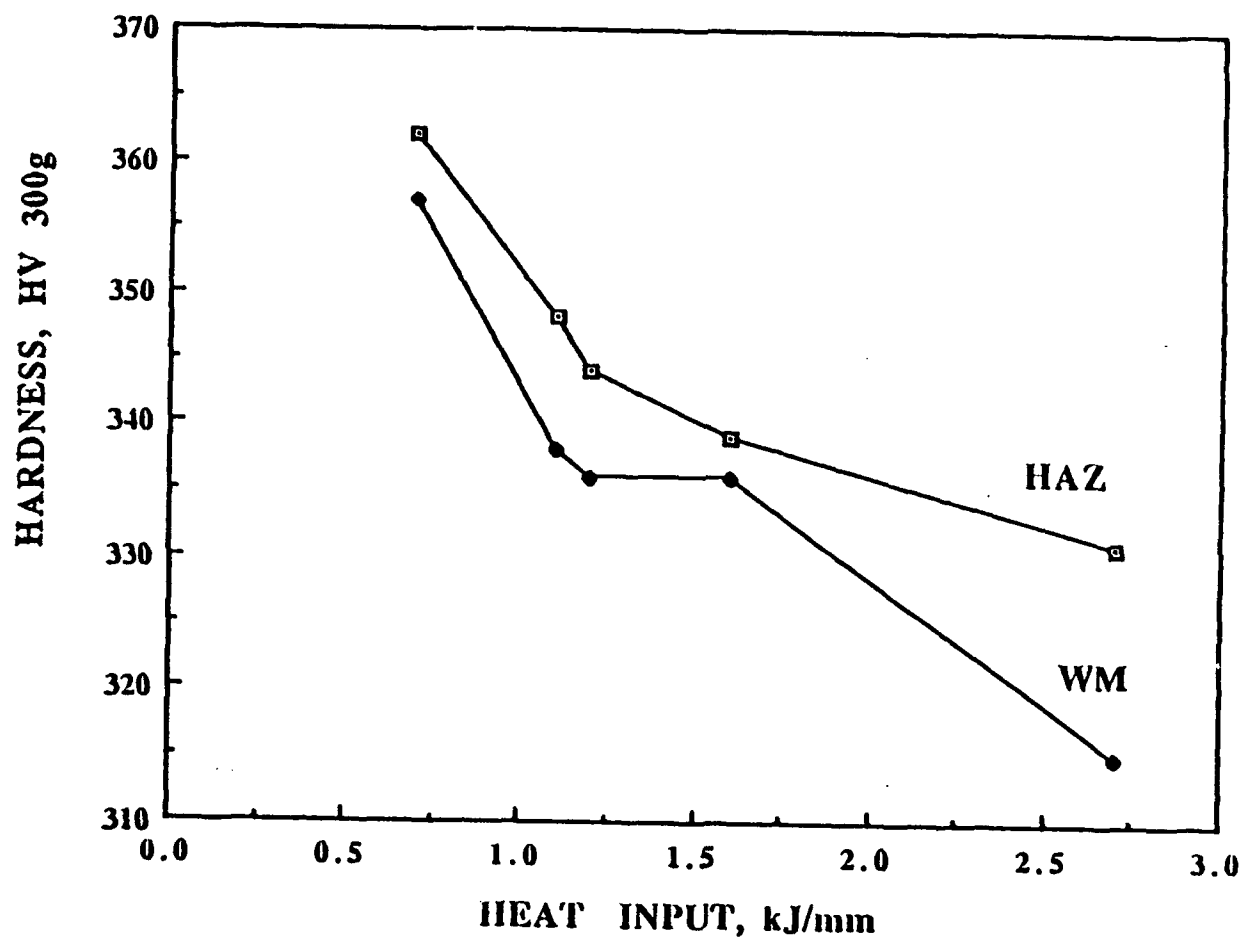
Figure 4. Peak hardnesses for both weld metals and HAZs as a function of heat input for all welds.
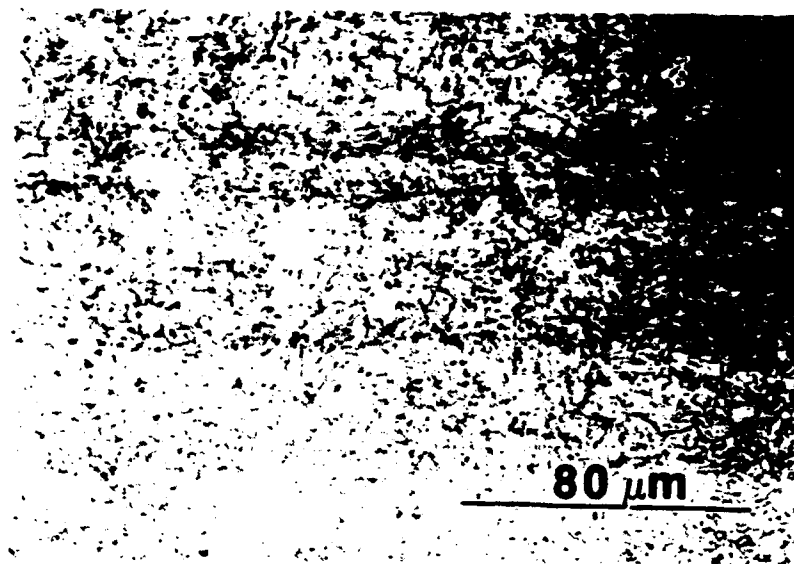
Figure 5. Optical micrograph of the as-received plate showing typical bainite/martensite 'packet' microstructure.
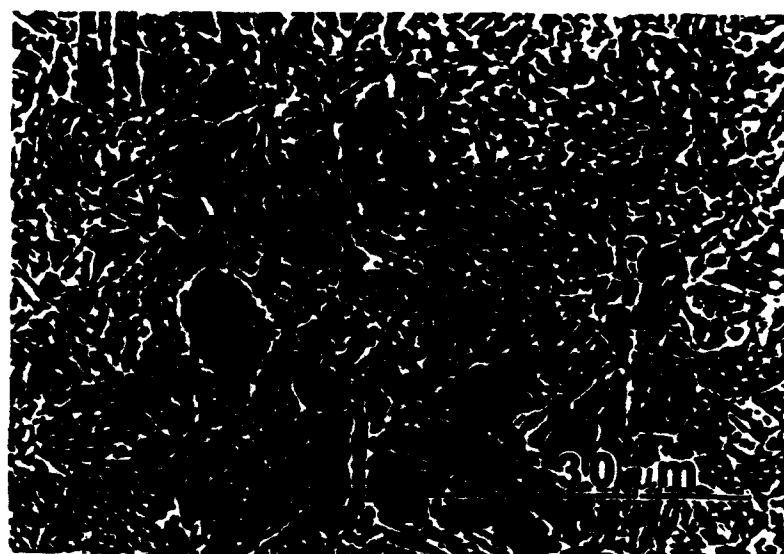
Figure 6. Backscattered electron SEM micrograph of the as-received plate showing more clearly, and at higher magnification, the features of figure 5.

12

Figure 7. TEM micrograph of as-received plate showing tempered granular bainite microstructure and ε-copper precipitates due to overaging.

13
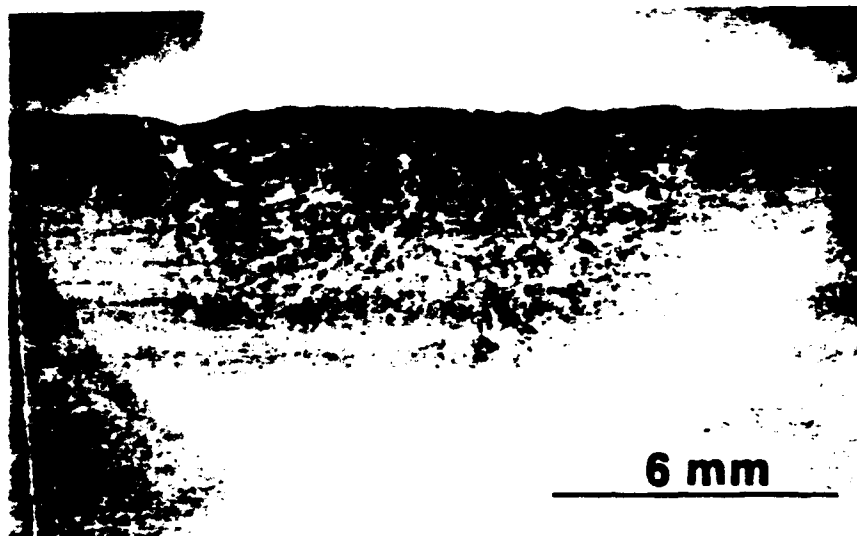
Figure 8. Low magnification optical micrograph of weld 1 (heat input = 2.7 kJ/mm)

Figure 9. Low magnification optical micrograph of weld 3 (heat input = 1.2 kJ/mm). Note hardness indentations.
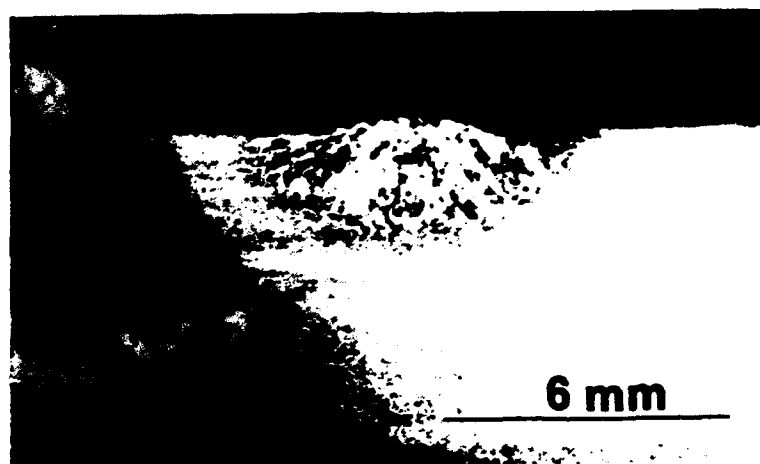

Figure 10. Low magnification optical micrograph of weld 5 (heat input = 0.7 kJ/mm). Note hardness intentations.
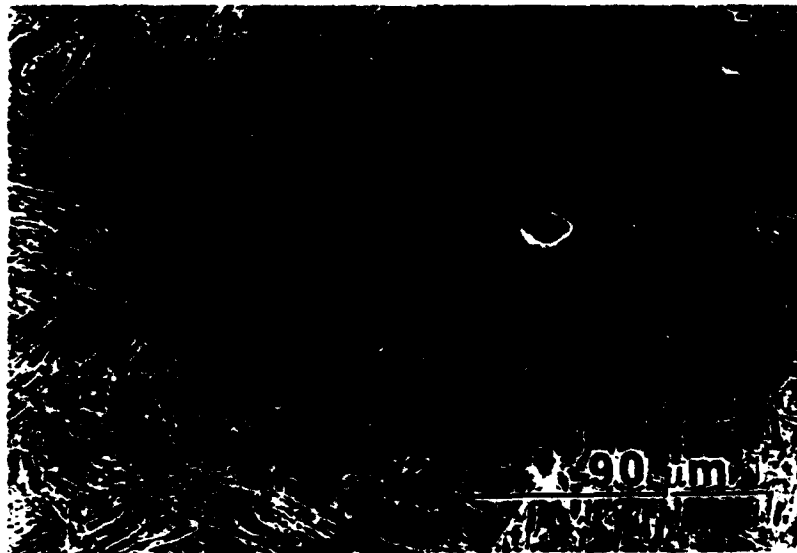
14

Figure 11. Secondary electron SEM micrograph of the HAZ next to the fusion zone boundary in weld 1 (heat input = 2.7 kJ/mm).
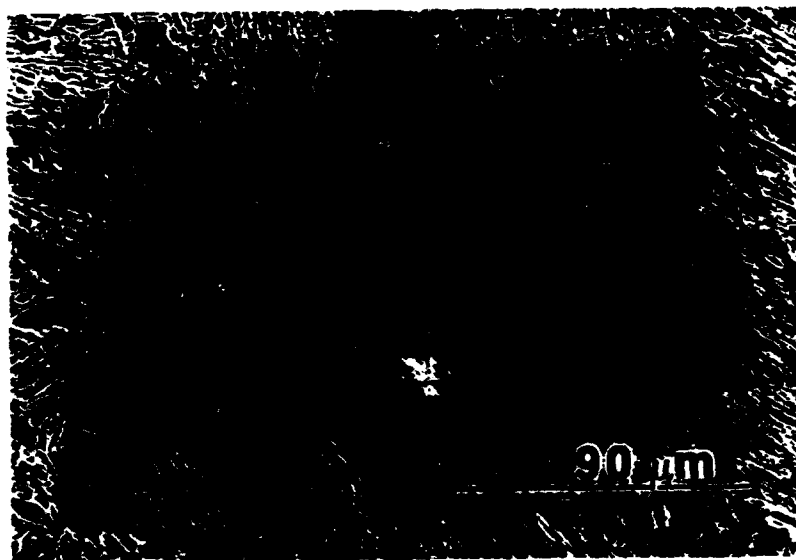

Figure 12. Secondary electron SEM micrograph of the HAZ next to the fusion zone boundary in weld 5 (heat input = 0.7 kJ/mm).
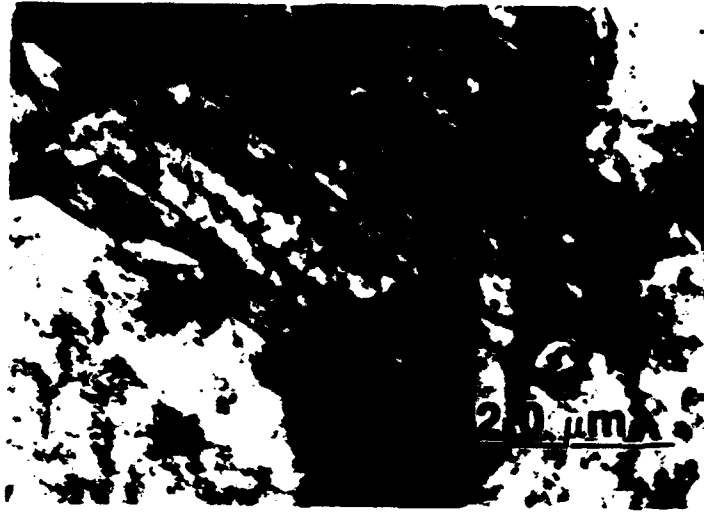
Figure 13. TEM micrograph of the HAZ next to the fusion zone boundary in weld 1 (heat input = 2.7 kJ/mm). The microstructure is granular bainite as evidenced by the presence of both 'blocky' and interlath retained austenite, the presence of both bainite and martensite laths and the 'equiaxed' nature of the features.

Figure 14. TEM micrograph of the HAZ next to the fusion zone boundary in weld 5 (heat input 0.7 kJ/mm). The microstructure is predominantly lath martensite with interlath retained austenite with some large bainite laths.
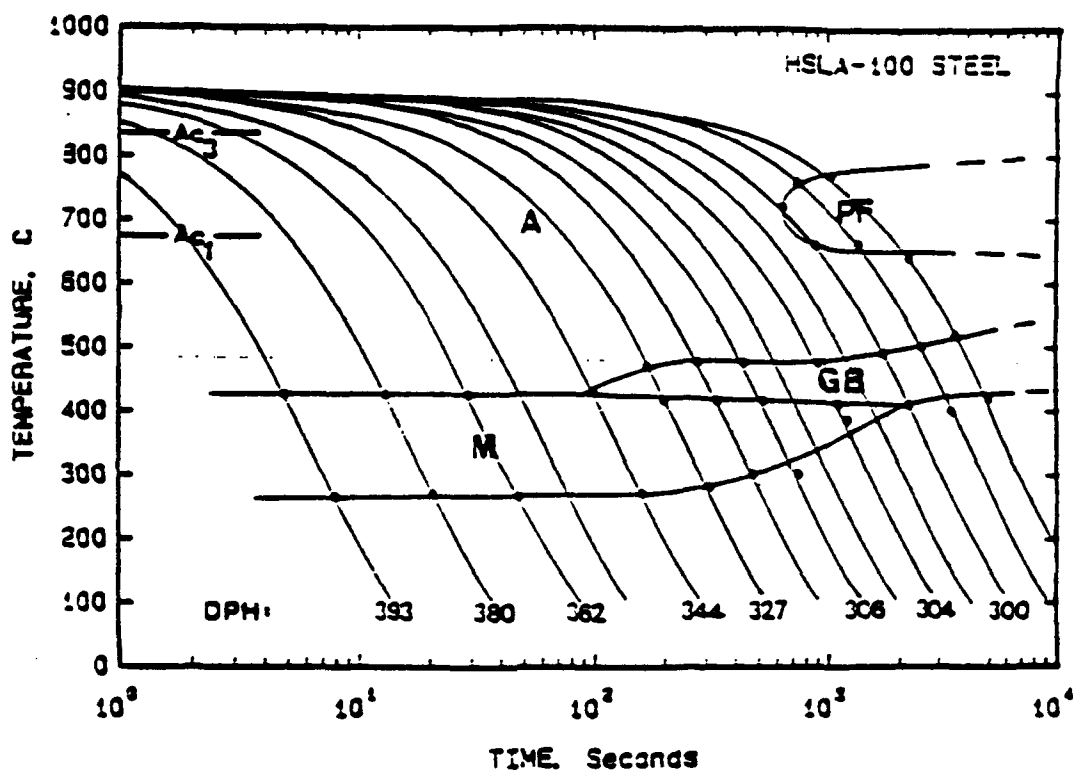
16

Figure 15. CCT diagram for a HSLA-100 steel with composition similar to that of the present work from Wilson, Hamburg, Colvin, Thompson and Krauss   (1988).

Distribution List

Agency	Number of Copies
Dudley Knox Library, Code 52 Naval Postgraduate School Monterey, CA 93943	2
Office of Research Administration, Code 08 Naval Postgraduate School Monterey, CA 93943	1
Dr M.G. Vassilaros, Code 2815 Annapolis Detachment, Carderock Division Naval Surface Warfare Center Annapolis, MD 21402	1
Mr .E.J. Czyryca, Code Annapolis Detachment, Carderock Division Naval Surface Warfare Center Annapolis, MD 21402	1
Mr G. Franke, Code 2815 Annapolis Detachment, Carderock Division Naval Surface Warfare Center Annapolis, MD 21402	1
Mr J. DeLoach, Code 2815 Annapolis Detachment, Carderock Division Naval Surface Warfare Center Annapolis, MD 21402	1
Mr Rick Wong, Code 2815 Annapolis Detachment, Carderock Division Naval Surface Warfare Center Annapolis, MD 21402	1
Mr P. Holzberg, Code 2815 Annapolis Detachment, Carderock Division Naval Surface Warfare Center Annapolis, MD 21402	1
Mr I Caplan, Code Annapolis Detachment, Carderock Division Naval Surface Warfare Center Annapolis, MD 21402	1
Professor A.G. Fox, Code ME/Fx Materials Science Section, Department of Mechanica Engineering United States Naval Postgraduate School Monterey, CA 93943	4
Defense Technical Information Center Cameron Station Alexandria, VA 22314	2